

3,4-Dihydroxyacetophenone attenuates oxidative stress-induced damage to HUVECs via regulation of the Nrf2/HO-1 pathway

DAIHONG CAO^{1*}, YUNHAN WANG^{1*}, WENTAO LI¹, JIAFEN JI²,
JUNTANG GUO¹, DAIJUAN ZHANG¹ and JIANGYUE LIU¹

¹Department of Pathophysiology, Weifang Medical University; ²Department of Pediatrics, Affiliated Hospital of Weifang Medical University, Weifang, Shandong 261053, P.R. China

Received December 28, 2021; Accepted April 4, 2022

DOI: 10.3892/mmr.2022.12715

Abstract. It has been reported that oxidative stress plays a prominent role in diabetic macrovascular diseases. 3,4-Dihydroxyacetophenone (3,4-DHAP) has been found to have a variety of biological activities. However, few studies have assessed the antioxidant capacity of 3,4-DHAP and the underlying mechanisms. Thus, the aim of the present study was to explore the effects of 3,4-DHAP on oxidative stress in human umbilical vein endothelial cells (HUVECs). HUVECs were pre-treated with 3,4-DHAP and then exposed to high glucose conditions. Cell viability and cytotoxicity were measured using an MTT assay. Reactive oxygen species (ROS) levels were measured using an inverted fluorescence microscope and a fluorescent enzyme labeling instrument. Protein expression levels of nuclear factor E2-related factor 2 (Nrf2), heme oxygenase-1 (HO-1), microtubule-associated protein 1A/1B-light chain 3 (LC3) and poly ADP-ribose polymerase-1 (PARP-1) were measured using western blotting, and mRNA expression of Nrf2 and HO-1 were measured through reverse transcription-quantitative PCR (RT-qPCR). Nrf2 nuclear translocation was evaluated using immunofluorescence analysis and autophagosomes were observed using transmission electron microscope (TEM). The results of the present study demonstrated that compared with the control group, cell viability of the high glucose group was reduced and cell cytotoxicity of the high glucose group was increased. ROS production in the high glucose group was clearly enhanced. In addition, high glucose upregulated Nrf2 and HO-1 protein

and mRNA expression levels. Nuclear translocation of Nrf2 in the high glucose group was also increased. The formation of autophagosomes in the high glucose group was also higher than that in the control group. Furthermore, LC3-II/LC3-I and PARP-1 protein expression levels were increased after treatment with high glucose. However, compared to the high glucose group, 3,4-DHAP (10 μ mol/l) significantly enhanced cell viability. 3,4-DHAP markedly decreased the production of ROS, increased Nrf2 and HO-1 protein and mRNA expression levels, and promoted nuclear translocation of Nrf2 in HUVECs. In addition, 3,4-DHAP promoted the formation of autophagosomes, and notably increased the protein expression levels of LC3-II/LC3-I and PARP-1. Moreover, it was determined that compared to the 3,4-DHAP group, treatment with 3,4-DHAP and ML385 enhanced cell viability, and decreased ROS production, Nrf2 and HO-1 protein and mRNA expression levels, nuclear translocation of Nrf2, and LC3-II/LC3-I and PARP-1 protein expression levels. Collectively, the results of the present study showed that 3,4-DHAP protected HUVECs against oxidative stress via regulation of the Nrf2/HO-1 pathway, by increasing autophagy and promoting DNA damage repair.

Introduction

Type 2 diabetes mellitus (T2DM), one of the most common and fastest growing diseases worldwide, is an endocrine and metabolic disease. It is estimated that 693 million adults will have T2DM by 2045 (1). The vascular complications of T2DM are some of the most important and pressing concerns in patients (2). In addition, the leading cause of death in diabetic patients is cardiovascular disease. Atherosclerosis constitutes the primary pathological outcome following the development of macrovascular complications, and it causes the thickening and hardening of the arterial wall and narrowing of the vascular lumen (3). Inflammation underlies the pathogenesis of atherosclerosis, which is the most common cause of cardiovascular disease (CVD) (4). The association between oxidative stress and inflammation has garnered growing interest in the study of the progression of the disease (5). Inflammation leads to increased ROS levels, which can induce oxidative stress (6). However, when the physiological antioxidant defense system is overwhelmed, excessive levels of ROS can lead to oxidative

Correspondence to: Professor Daijuan Zhang or Professor Jiangyue Liu, Department of Pathophysiology, Weifang Medical University, 7166 Baotong West Street, Weifang, Shandong 261053, P.R. China
E-mail: wxy070604@126.com
E-mail: jiangyue7879@126.com

*Contributed equally

Key words: 3,4-dihydroxyacetophenone, antioxidation, oxidative stress, autophagy, nuclear factor E2-related factor 2

stress (7). Therefore, there is an urgent need to discover novel treatments to prevent and treat the diabetes-associated macrovascular diseases.

High concentrations of glucose can promote apoptosis of endothelial cells, which is closely related to vascular complications. In addition, high glucose conditions can not only cause metabolic disorders, but also produce excess quantities of oxygen-free radicals, resulting in oxidative stress, which in-turn results in toxic effects on endothelial cells, and this process plays an important role in the development of atherosclerosis, a vascular complication of diabetes. Therefore, in the present study HUVECs cultured under high glucose conditions were used as a model to study the antioxidant effect of 3,4-DHAP.

Cellular antioxidant defense plays a crucial role in protecting against oxidative stress (8). Nuclear factor E2-related factor 2 (Nrf2) is the major transcriptional regulator of antioxidant gene expression (9). Nrf2 participates in the pathogenesis of several diseases (10-13). Under physiological conditions, Nrf2 forms a complex with Keap1, thereby mediating Nrf2 proteasomal degradation and ubiquitination (14). However, when subjected to oxidative stress or other physiological stimuli, Nrf2 cannot interact with Keap1, resulting in Nrf2 activation, nuclear translocation and transcription of downstream genes of the Nrf2 transcription factor, including heme oxygenase-1 (HO-1) (15). Increased production of ROS disassociates Nrf2 from Keap1, and Nrf2 translocates to the nucleus in the dissociated form, where it results in transcription of several genes (16). Nrf2 protects cells against oxidative stress by activating several signaling pathways. HO-1 is a critical antioxidant enzyme regulated by Nrf2 (17). Zhang *et al.* (18) indicated that the Nrf2/HO-1 signaling pathway was activated under conditions of increased ROS. Ci *et al.* (19) demonstrated that farrerol decreased oxidative stress through activation of Nrf2 to induce HO-1 expression. Mohammad *et al.* (20) also showed that HO-1 was upregulated in response to oxidative stress. Thus, the Nrf2/HO-1 pathway has become a research hotspot in recent years.

Similar to the Nrf2 pathway, autophagy plays a role in cell homeostasis when stimulated by oxidative stress (21). Autophagy, which includes macro-autophagy, micro-autophagy and chaperone-mediated autophagy, is a process of regulated cellular degradation (22). During autophagy, autophagosomes 'swallow' cytoplasmic proteins or organelles and fuse with lysosomes to form autophagic lysosomes, and the components of the autophagosome are degraded by the contained lysosomal hydrolases (23). Microtubule-associated protein 1A/1B-light chain 3 (LC3) is a marker of autophagy. It is primarily involved in the formation of autophagosomes. LC3 also plays a role in mitochondrial autophagy, regulating the quantity of mitochondria by eliminating them to minimal levels required to meet the immediate energy demands of the cell and prevent excessive ROS production (24). The autophagy of mitochondria is primarily initiated by PTEN-induced putative kinase 1 (PINK1). PINK proteins degrade cellular components through the actions of presenilin-associated rhomboid-like (PARL) under physiological conditions, whereas the function of PARL is inhibited when the mitochondria are damaged, and in this situation, PINK stabilizes and recruits Parkin, the E3 ligase, to initiate autophagy (25). Concurrently, the cytoplasmic form of LC3 (LC3-I) binds to phosphatidylethanolamine to form

LC3 phosphatidylethanolamine conjugate (LC3-II), which is recruited to the autophagic membrane. The formation of autophagosomes is the basis of autophagy and affects the transformation of LC3-I to LC3-II (26). Hence, LC3 expression is accepted as a marker for autophagy. When the autophagic process is initiated, LC3-I is transformed into LC3-II and this commits the cell to undergoing autophagy (27).

DNA, the genetic material of eukaryotic cells, is damaged every day by a variety of internal and external factors. When the DNA is damaged, DNA damage repair pathways are activated to ensure the stability of the genome. Reactive oxygen species (ROS) are a factor that can cause DNA damage. PARP is a DNA damage response sensor. PARP-1, the cleavage substrate of caspase, is also involved in DNA repair, gene expression regulation, genomic stability and apoptosis (28,29). A previous study has shown that PARP-1 plays crucial roles in DNA cell repair and survival using PARP-1 knockout mice (30). Another study has also shown that PARP-1 regulates DNA repair factor availability, and this is an attractive target in the study of cancer therapeutics (31). Pazzaglia and Pioli (32) showed that PARP exerted a protective role in DNA repair and regulated inflammatory processes. Moreover, it has been shown that autophagy may be cytoprotective in response to DNA repair, via regulation of PARP-1 activation (33). Wang *et al.* (34) determined that farrerol could ameliorate hepatotoxicity induced by PARP-1, and this was achieved through activation of Nrf2 and induction of autophagy. Therefore, whether 3,4-dihydroxyacetophenone (3,4-DHAP) could protect HUVECs against high glucose-induced damage via regulating PARP-1 was assessed in the present study.

3,4-DHAP is an active ingredient from *Ilex glauca* leaves and has a variety of beneficial biological activities, including anti-inflammatory, antioxidative and cardioprotective properties (35), and has been shown to suppress melanin production (36), inhibit platelet aggregation, promote coronary artery dilation and improve blood circulation (37). In our previous study, it was shown that 3,4-DHAP reduced the levels TNF- α secretion from RAW264.7 cells, thus exhibiting an anti-inflammatory effect. It was also shown that 3,4-DHAP decreased the levels of inflammation-related indicators in a rabbit model of atherosclerosis induced by hypercholesterolemia (38). However, the effects of 3,4-DHAP on oxidative stress and its underlying mechanism remain to be assessed. Therefore, the aim of the present study was to investigate whether 3,4-DHAP could protect HUVECs against oxidative stress via regulation of the Nrf2/HO-1 signaling pathway, and the effects on autophagy and DNA damage repair in this process.

Materials and methods

Reagents. 3,4-DHAP was purchased from Jinan Luxin Chemical Technology Co., Ltd. Sulforaphane (SFN), an antioxidant reagent that was used as a positive control, was obtained from Sigma-Aldrich; Merck KGaA. ML385, a novel and specific Nrf2 inhibitor, was purchased from Selleck Chemicals. ML385 is an inhibitor of Nrf2 activity and nuclear translocation, which has been confirmed to affect the expression of downstream genes. The ROS assay kit, Nuclear and Cytoplasmic Protein Extraction Kit, double antibiotics, MTT

kit, DAPI and Fluorescent Mounting Media were obtained from Beijing Solarbio Science & Technology Co., Ltd.

Cell culture. HUVECs were obtained from Shanghai Baili Biotechnology (produced by ATCC). The HUVECs used were an immortalized cell line. The cells were cultured in DMEM (Gibco; Thermo Fisher Scientific, Inc.) supplemented with 15% FBS (EVERY GREEN; Zhejiang Tianhang Biotechnology, Co., Ltd.) and 1% penicillin/streptomycin (Beijing Solarbio Science & Technology Co., Ltd.) at 37°C, in a humidified incubator supplied with 5% CO₂. HUVECs were randomly grouped according to the experimental design as follows: Control group, high glucose group, SFN group (SFN + high glucose), 3,4-DHAP group (3,4-DHAP + high glucose), and 3,4-DHAP + ML385 group (3,4-DHAP + ML385 + high glucose). The cells were pretreated with SFN (20 μmol/l), 3,4-DHAP (10 μmol/l) or ML385 (0.25 μmol/l) for 6 h, then exposed to high glucose conditions (33.3 mmol/l) for 12 h.

MTT assay. For assessment of cell viability and cytotoxicity, an MTT assay was performed. The HUVECs were evenly plated on a 96-well cell culture plate with ~5,000 cells/well and cultured at 37°C for 24 h. HUVECs were pretreated with 1, 10, 20, 50 or 100 μmol/l 3,4-DHAP, after which, the OD values were measured. The cells were pretreated with 20 μmol/l SFN and 10 μmol/l 3,4-DHAP for 6 h and then cultured at 37°C with 33.3 mmol/l glucose for 12 h. Subsequently, to each well, 10 μl MTT solution was added (5 mg/ml), and cells were incubated for a further 4 h. Finally, the supernatant was discarded, the resulting blue-purple crystals were dissolved using 150 μl DMSO with shaking for 10 min. Using a microplate reader, the absorbance of each well was measured at 490 nm. Cell viability was calculated, and a histogram was created.

ROS activity. The ROS levels are the most commonly detected indicator of oxidative stress. HUVECs were plated in a 6-well plate at a density of 1x10⁵ cells/well. After treatment as described above, the cells were washed with PBS. DCFH-DA was added to each well, and incubated at 37°C for 30 min in dark. The ROS levels were measured using a fluorescent enzyme label instrument (Spectra Max M5; Molecular Devices LLC). Images were obtained using an Inverted Fluorescence Microscope (Olympus Corporation).

Western blot analysis. Total protein from cells in each group was collected using RIPA lysis buffer (Beijing Solarbio Science & Technology Co., Ltd.). The cytoplasmic and the nuclear proteins were separately acquired using a Nuclear and Cytoplasmic Protein Extraction Kit according to the manufacturer's instructions. A BCA assay kit was used to measure the protein concentration. According to the protein concentration, the amount of sample protein (40 μg) was calculated and separated by 10 or 12% SDS-PAGE. When the electrophoresis had finished, a strip of gel was cut and this was used to transfer proteins to a PVDF film. The PVDF film containing the protein of interest was immersed in 5% skimmed milk powder at 37°C for 2 h, washed three times with TBST (0.05% Tween-20; 10 min each), and incubated with one of the following primary antibodies: Nrf2 (1:1,000; cat. no. SAB4501984; Sigma-Aldrich; Merck KGaA), HO-1 (1:25,000; cat. no. ab68477; Abcam), LC3

(1:1,000; cat. no. ab192890; Abcam) and PARP-1 (1:2,500; cat. no. ab32138; Abcam) at 4°C overnight. Then the PVDF film was washed with TBST and incubated with a secondary antibody: GAPDH (1:7,000; cat. no. AF1186; Beyotime Institute of Biotechnology) or H3 (1:2,000; cat. no. ab32356; Abcam) at 37°C for 1 h. The PVDF film was treated with an enhanced chemiluminescence reagent (Beijing Solarbio Science & Technology Co., Ltd.), and the signals were visualized using a chemiluminescence detection system (FluorChem E; Protein Simple Ltd.). Quantitative expression of proteins was calculated using ImageJ software (v1.8.0; National Institutes of Health).

Reverse transcription-quantitative PCR (RT-qPCR). According to the manufacturer's instructions, the RNA of HUVECs was extracted by lysing cells on ice using TRIzol[®] reagent (Beijing ComWin Biotech Co., Ltd.), and then reverse transcribed into cDNA using the ReverTra Ace qPCR RT Kit [cat. no. FSQ-101; Toyobo (Shanghai) Biotech, Co., Ltd.]. qPCR was performed using SYBR[®] Green Real-time PCR Master Mix (cat. no. QPK-201; Toyobo (Shanghai) Biotech, Co., Ltd.) in a 7500 Sequence Detection System. The thermocycling conditions were as follows: Initial denaturation at 95°C for 60 sec; followed by 40 cycles at 95°C for 15 sec, 60°C for 15 sec and 72°C for 45 sec. The primer sequences used were: Nrf2 forward, 5'-CCC AGCACATCCAGTCAGAAACC-3' and reverse, 5'-AGCCGA AGAAACCTCATTGTCTACTAC-3'; HO-1 forward, 5'-TGC CAGTGCCACCAAGTTCAAG-3' and reverse, 5'-TGTTGA GCAGGAACGCAGTCTTG-3'; and GAPDH forward, 5'-CAG GAGGCATTGCTGATGAT-3' and reverse, 5'-GAAGGCTGG GGCTCATTT-3'. All mRNA expression levels were normalized to the housekeeping gene GAPDH. Relative expression was calculated using the 2^{-ΔΔC_q} method (39).

Cellular immunofluorescence. After discarding the culture medium, the cells were washed with PBS three times (5 min each). Formaldehyde (2%) was added and cells were fixed at 37°C for 30 min, after which, the solution was removed, cells were washed with PBS three times (5 min each) permeabilized using 0.3% Triton X-100 at 37°C for 15 min, washed as above, blocked using 10% goat serum at 37°C for 2 h, incubated with the Nrf2 primary antibody (1:100; cat. no. SAB4501984; Sigma-Aldrich) overnight at 4°C, washed, incubated with the secondary FITC-conjugated antibody (1:100; cat. no. ZF-0311; ZSGB-BIO; OriGene Technologies, Inc.) in the dark at 37°C for 1 h, washed, stained with DAPI at 37°C for 5 min, then washed again. The cell climbing piece (Thermo Fisher Scientific, Inc.) and coverslip were removed and sealed using the Fluorescent Mounting Media. Images were obtained using a fluorescence microscope (magnification, x10; Olympus Corporation).

Assessment of autophagosome formation. After treating cells as described above, the cells were collected, centrifuged at 1,006.2 x g for 10 min, fixed with 3% glutaraldehyde at 4°C for 12 h, fixed with 1% osmic acid at 37°C for 2 h, and embedded using pure embedding solution for 2 h. The samples were dehydrated in a series of increasing ethanol solutions, embedded and set in epoxy resin at different temperatures and for different lengths of times (37°C for 12 h, 45°C for 12 h and 60°C for 24 h). The embedded samples were cut into ultra-thin

sections (70 nm), and then stained (3% uranium acetate for 15-30 min and lead citrate for 5-10 min, at 37°C). Finally, the images were captured using a transmission electron microscope (magnification, x5,000).

Statistical analysis. All data were analyzed using GraphPad Prism version 7.0 (GraphPad Software, Inc.). Results are presented as the mean \pm SD. Unpaired Student's t-tests were used for comparisons between two groups. Comparisons among multiple groups were analyzed using one-way ANOVA followed by Tukey's post hoc test. $P < 0.05$ was considered to indicate a statistically significant difference.

Results

3,4-DHAP increases cell viability and reduces cytotoxicity. The cell viability of HUVECs was assessed using an MTT assay. The basic principle is that the amber dehydrogenase in the mitochondria of living cells can reduce the exogenous MTT, causing it to crystallize and deposit the blue-purple formazan, which is difficult to dissolve in water in living cells, while the dead cells have no such function. In Fig. 1A, compared with the control group, in cells treated with 10 $\mu\text{mol/l}$ 3,4-DHAP, the cell viability was increased ($P < 0.01$); the cell viability of 3,4-DHAP when treated with 1, 20 and 50 $\mu\text{mol/l}$ 3,4 DHAP was reduced ($P < 0.05$); and the cell viability when treated with 100 $\mu\text{mol/l}$ 3,4-DHAP was also reduced ($P < 0.001$). Thus, 10 $\mu\text{mol/l}$ 3,4-DHAP was selected for subsequent experiments. In Fig. 1B, the cell viability of the high glucose group was significantly reduced compared with the control group ($P < 0.001$), and this demonstrated that a successful *in vitro* model of diabetes had been established. The cell viability was significantly increased after pretreatment with SFN ($P < 0.01$) and 3,4-DHAP ($P < 0.001$), and there was significant difference between the SFN group and the 3,4-DHAP group ($P < 0.01$). Compared to the 3,4-DHAP group, the cell viability in the 3,4-DHAP + ML385 group was reduced ($P < 0.05$). These results indicated that 3,4-DHAP could protect HUVECs from high glucose-induced cell death.

3,4-DHAP reduces ROS levels in HUVECs. Intracellular ROS levels were determined using a fluorescent enzyme labeling instrument. ROS levels were detected using the fluorescent probe DCFH-DA. DCFH-DA does not fluoresce itself and can pass through the cell membrane freely. After entering the cell, DCFH can be hydrolyzed by esterases in the cell to generate DCFH. DCFH cannot penetrate a cell membrane, making it easy to probe in loaded cells. Intracellular ROS can oxidize non-fluorescent DCFH to generate fluorescent DCF, and the fluorescence of DCF can be detected to determine the levels of intracellular ROS (40). As shown in Fig. 2A, compared with the control group, the high glucose group exhibited significantly increased ROS production ($P < 0.001$); compared with the high glucose group, SFN and 3,4-DHAP group significantly reduced the production of ROS ($P < 0.001$), but there was no significant difference between the SFN group and the 3,4-DHAP group ($P > 0.05$). Compared with the 3,4-DHAP group, the ROS levels in the 3,4-DHAP + ML385 group were increased ($P < 0.01$). In Fig. 2B, compared with the control group, the

high glucose group significantly increased fluorescence intensity ($P < 0.001$); compared with the high glucose group, the SFN and 3,4-DHAP groups significantly reduced the fluorescence intensity ($P < 0.01$), but there was no significant difference between the SFN group and the 3,4-DHAP group ($P > 0.05$). Compared with the 3,4-DHAP group, fluorescence intensity in the 3,4-DHAP + ML385 group was increased ($P < 0.05$). The fluorescent images also showed corroborating results (Fig. 2C). These findings suggested that 3,4-DHAP could attenuate the oxidative stress induced by high glucose conditions in HUVECs.

3,4-DHAP upregulates Nrf2 protein and mRNA expression levels. As shown in Fig. 3A and B, Nrf2 total protein expression in the high glucose group was increased compared with the control group ($P < 0.001$). Compared to the high glucose group, Nrf2 total protein expression was increased in the SFN group ($P < 0.05$). Nrf2 total protein expression in the 3,4-DHAP group was also significantly increased compared to the high glucose group ($P < 0.01$). The total Nrf2 protein expression in the 3,4-DHAP group was higher than that in the SFN group, but there was no significant difference between these groups ($P > 0.05$). Compared with the 3,4-DHAP group, the total Nrf2 protein expression in the 3,4-DHAP + ML385 group was significantly reduced ($P < 0.05$). In Fig. 3C, the mRNA expression level of Nrf2 in the high glucose group was increased compared with the control group ($P < 0.05$). Compared with the high glucose group, Nrf2 mRNA expression was increased in the SFN group ($P < 0.05$). Nrf2 mRNA expression in the 3,4-DHAP group was also significantly increased compared with the high glucose group ($P < 0.001$). Nrf2 mRNA expression in the 3,4-DHAP group was significantly higher than that in the SFN group, and the difference was significant ($P < 0.01$). Compared to the 3,4-DHAP group, the mRNA expression level of Nrf2 in the 3,4-DHAP + ML385 group was significantly reduced ($P < 0.001$). These findings indicated that 3,4-DHAP could protect HUVECs against oxidative stress, and this may have been regulated by the Nrf2 pathway.

3,4-DHAP increases Nrf2 nuclear translocation. Nrf2 nuclear protein expression is shown in Fig. 4A. The nuclear translocation of Nrf2 was reduced when cells were exposed to oxidative stress. As shown in Fig. 4B, compared with the control group, the high glucose group exhibited slightly increased Nrf2 nuclear protein expression ($P < 0.05$). Nrf2 nuclear protein expression increased when pretreated with SFN ($P > 0.05$) and 3,4-DHAP ($P < 0.01$) compared with the high glucose group, and the difference between the SFN and the 3,4-DHAP group was also significant ($P < 0.05$). Compared with the 3,4-DHAP group, the nuclear expression of Nrf2 in the 3,4-DHAP + ML385 group was decreased ($P < 0.001$). In Fig. 4C and D, the fluorescence intensity of the high glucose group was higher than that of control group ($P < 0.001$). Compared with the high glucose group, the fluorescence intensity of the SFN group was increased ($P < 0.05$), the fluorescence intensity of the 3,4-DHAP group was significantly also increased ($P < 0.01$), and the difference between the SFN and the 3,4-DHAP group was also significant ($P < 0.05$). Compared with the 3,4-DHAP group, the fluorescence intensity in the 3,4-DHAP + ML385

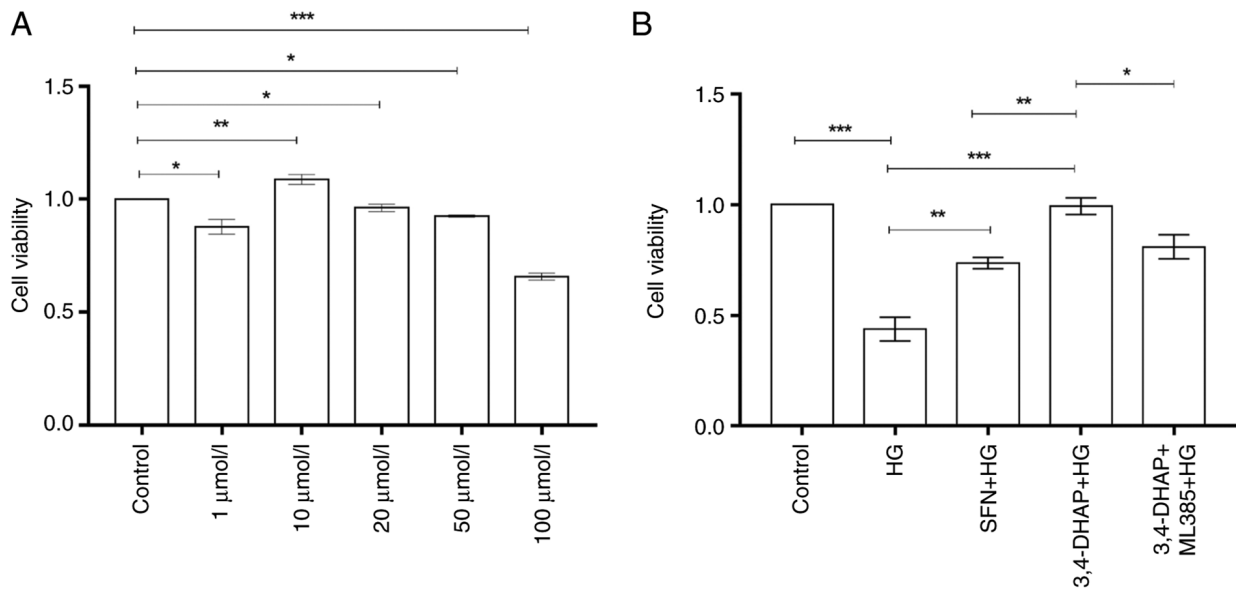


Figure 1. 3,4-DHAP increases cell viability and reduces cytotoxicity. (A) HUVEC viability following treatment with different concentrations of 3,4-DHAP. (B) HUVEC viability in the different treatments groups. Data are presented as the mean \pm SD of three repeats. * $P < 0.05$, ** $P < 0.01$ and *** $P < 0.001$. HUVEC, human umbilical vein endothelial cell; 3,4-DHAP, 3,4-dihydroxyacetophenone; HG, high glucose; SFN, sulforaphane.

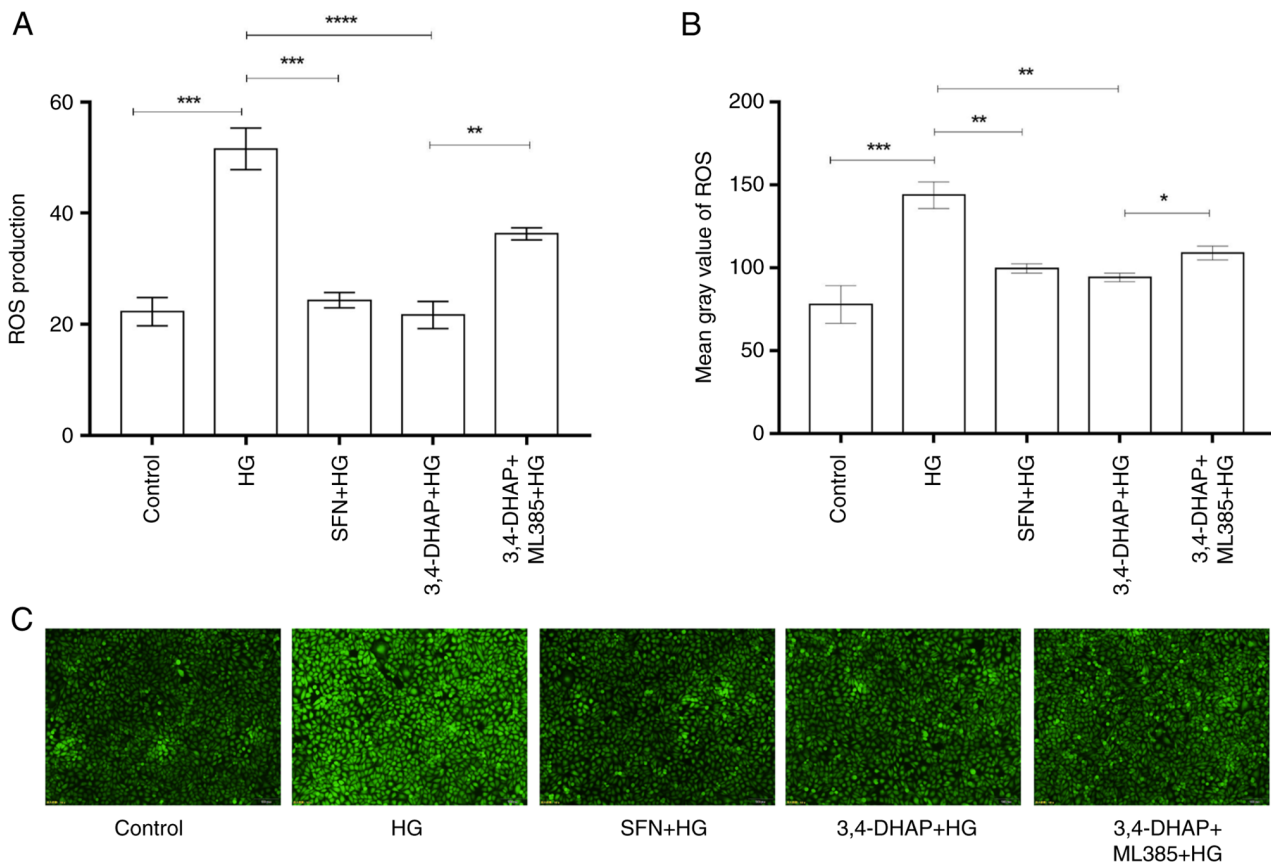


Figure 2. 3,4-DHAP reduces ROS activity in HUVECs. (A) ROS levels were measured using a fluorescent enzyme label instrument. (B) Mean gray values of ROS were measured using ImageJ software. (C) ROS were imaged using an inverted fluorescence microscope (magnification, $\times 10$). Data are presented as the mean \pm SD of three repeats. * $P < 0.05$, ** $P < 0.01$, *** $P < 0.001$ and **** $P < 0.0001$. 3,4-DHAP, 3,4-dihydroxyacetophenone; ROS, reactive oxygen species; HUVECs, human umbilical vein endothelial cells; HG, high glucose; SFN, sulforaphane.

group was decreased ($P < 0.0001$). These results showed that 3,4-DHAP exerted antioxidant effects by regulating Nrf2 nuclear translocation.

3,4-DHAP enhances HO-1 expression. Fig. 5A shows the protein expression levels of HO-1. As shown in Fig. 5B, HO-1 expression at the protein level in the high glucose group was

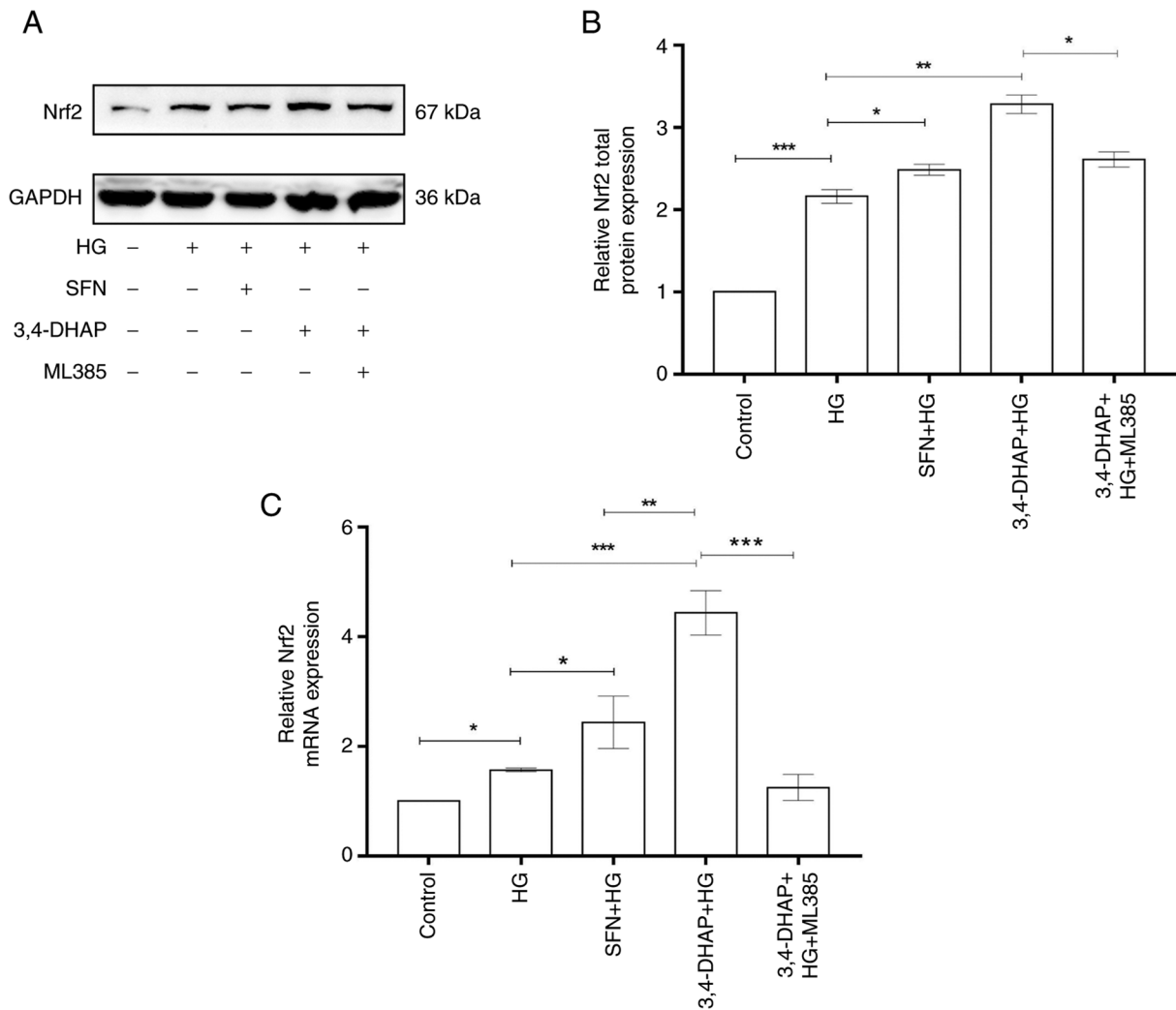


Figure 3. 3,4-DHAP upregulates Nrf2 protein and mRNA expression levels. (A) Nrf2 protein expression levels were measured by western blotting and (B) quantified using ImageJ software. (C) Nrf2 mRNA expression levels. Data are presented as the mean \pm SD of three repeats. * $P < 0.05$, ** $P < 0.01$ and *** $P < 0.001$. 3,4-DHAP, 3,4-dihydroxyacetophenone; Nrf2, nuclear factor E2-related factor 2; HG, high glucose; SFN, sulforaphane.

slightly increased compared with the control group ($P < 0.05$). Compared with the high glucose group, HO-1 protein expression was enhanced in the SFN group ($P < 0.05$). Compared with the high glucose group, 3,4-DHAP group also exhibited significantly increased expression of HO-1 ($P < 0.01$). HO-1 expression in the 3,4-DHAP group was higher than that in the SFN group, and there was no significant difference between the SFN and 3,4-DHAP groups ($P > 0.05$). HO-1 expression in the 3,4-DHAP + ML385 group was reduced compared with 3,4-DHAP group ($P < 0.001$). As shown in Fig. 5C, the mRNA expression level of HO-1 in the high glucose group was slightly increased compared with the control group ($P < 0.05$). Compared with the high glucose group, HO-1 mRNA expression levels were significantly increased in the SFN group ($P < 0.05$) and in the 3,4-DHAP group ($P < 0.001$). HO-1 mRNA expression in the 3,4-DHAP group was higher than that in the SFN group, and there was a significant difference between the SFN and 3,4-DHAP groups ($P < 0.01$). Compared to the 3,4-DHAP group, the mRNA expression levels of HO-1 in the 3,4-DHAP + ML385 group was decreased ($P < 0.001$). These findings further indicated that 3,4-DHAP could protect HUVECs from oxidative stress by regulating the Nrf2/HO-1 pathway.

3,4-DHAP upregulates LC3 protein expression. LC3 is considered to the primary indicator of autophagy (41). Fig. 6A shows LC3 protein expression. As shown in Fig. 6B, the protein expression ratio of LC3-II/LC3-I in the high glucose group was increased compared with the control group ($P < 0.05$). Compared with the high glucose group, the LC3-II/LC3-I ratio was increased in the SFN group ($P > 0.05$). Compared with the high glucose group, 3,4-DHAP markedly increased the LC3-II/LC3-I protein ratio ($P < 0.01$). The LC3-II/LC3-I ratio in the 3,4-DHAP group was higher than that in the SFN group, and the difference was significant ($P < 0.01$). Compared with the 3,4-DHAP group, the 3,4-DHAP + ML385 group exhibited a reduced LC3-II/LC3-I ratio ($P < 0.01$). These findings suggest that 3,4-DHAP can promote autophagy in response to oxidative stress induced by high glucose treatment in HUVECs.

3,4-DHAP promotes the formation of autophagosomes. Formation of autophagosomes was detected by TEM. Compared with the control group, the high glucose group exhibited a slight increase in autophagosome formation ($P < 0.05$). However, the formation of autophagosomes was evidently increased after SFN ($P < 0.05$) and 3,4-DHAP ($P < 0.01$) treatment compared

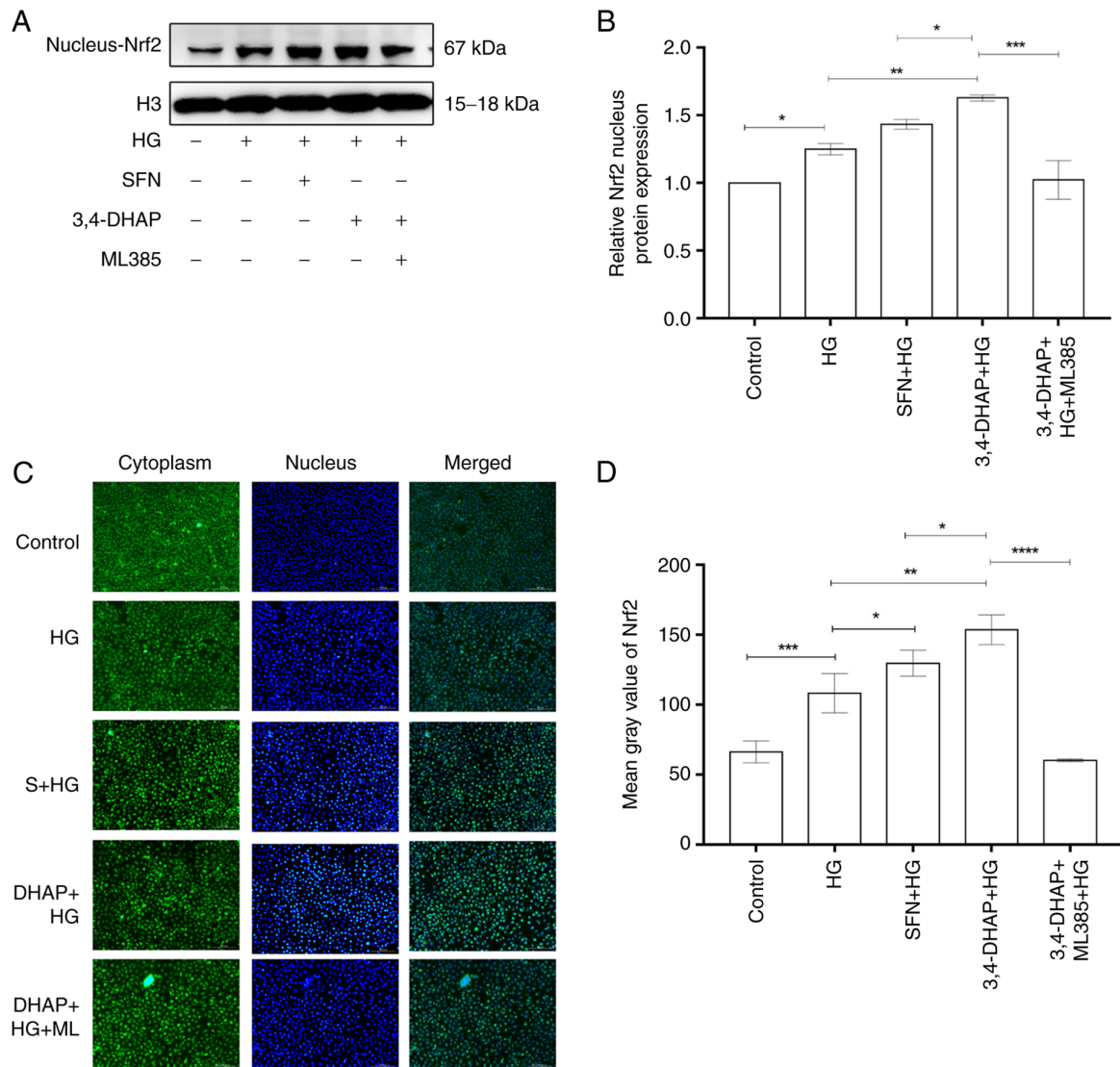


Figure 4. 3,4-DHAP promotes Nrf2 nuclear translocation. (A) Nrf2 nuclear protein expression levels were measured by western blotting and (B) quantified using ImageJ software. (C) Nrf2 protein expression levels in the cytoplasm and nucleus were imaged using an inverted fluorescence microscope (magnification, x10). (D) Mean gray values of ROS were measured using ImageJ software. Data are presented as the mean \pm SD of three repeats. * $P < 0.05$, ** $P < 0.01$, *** $P < 0.001$ and **** $P < 0.0001$. 3,4-DHAP, 3,4-dihydroxyacetophenone; Nrf2, nuclear factor E2-related factor 2; ROS, reactive oxygen species; HG, high glucose; SFN, sulforaphane.

with high glucose group, and there was a significant difference between the SFN and 3,4-DHAP groups ($P < 0.05$). Compared with the 3,4-DHAP group, the 3,4-DHAP + ML385 group exhibited decreased formation of autophagosomes ($P < 0.01$) (Fig. 7). The results further showed that 3,4-DHAP could promote autophagy in response to oxidative stress.

3,4-DHAP enhances PARP-1 protein expression. PARP-1 is a receptor for DNA damage response (42). Fig. 8A shows PARP-1 protein expression. As shown in Fig. 8B, the protein expression levels of PARP-1 in the high glucose group were increased compared with the control group ($P < 0.01$). Compared with the high glucose group, PARP-1 protein expression was increased in the SFN group ($P > 0.05$); 3,4-DHAP also significantly increased PARP-1 protein expression levels ($P < 0.001$). PARP-1 levels in the 3,4-DHAP group were higher than those in the SFN group, and the difference was significant ($P < 0.01$). Compared with the 3,4-DHAP group, the protein expression

levels of PARP-1 in the 3,4-DHAP + ML385 group were reduced ($P < 0.001$). These findings further demonstrated that 3,4-DHAP could promote the response to cell damage via regulation of PARP-1 expression.

Discussion

With the increasing adoption of unhealthy diets and improvements in living standards, the incidence of T2DM is increasing annually, posing a significant burden to the health and quality of life of individuals (43). Atherosclerosis, the most common complication of T2DM, is a chronic inflammatory disease (44). Endothelial dysfunction, the initial link in the early stage of atherosclerosis, is an early manifestation that occurs prior to the formation of atherosclerosis and affects the occurrence and development of atherosclerosis. Endothelial cells can be damaged by several factors, such as oxidative stress, proinflammatory factors, hyperglycemia, hyperlipidemia

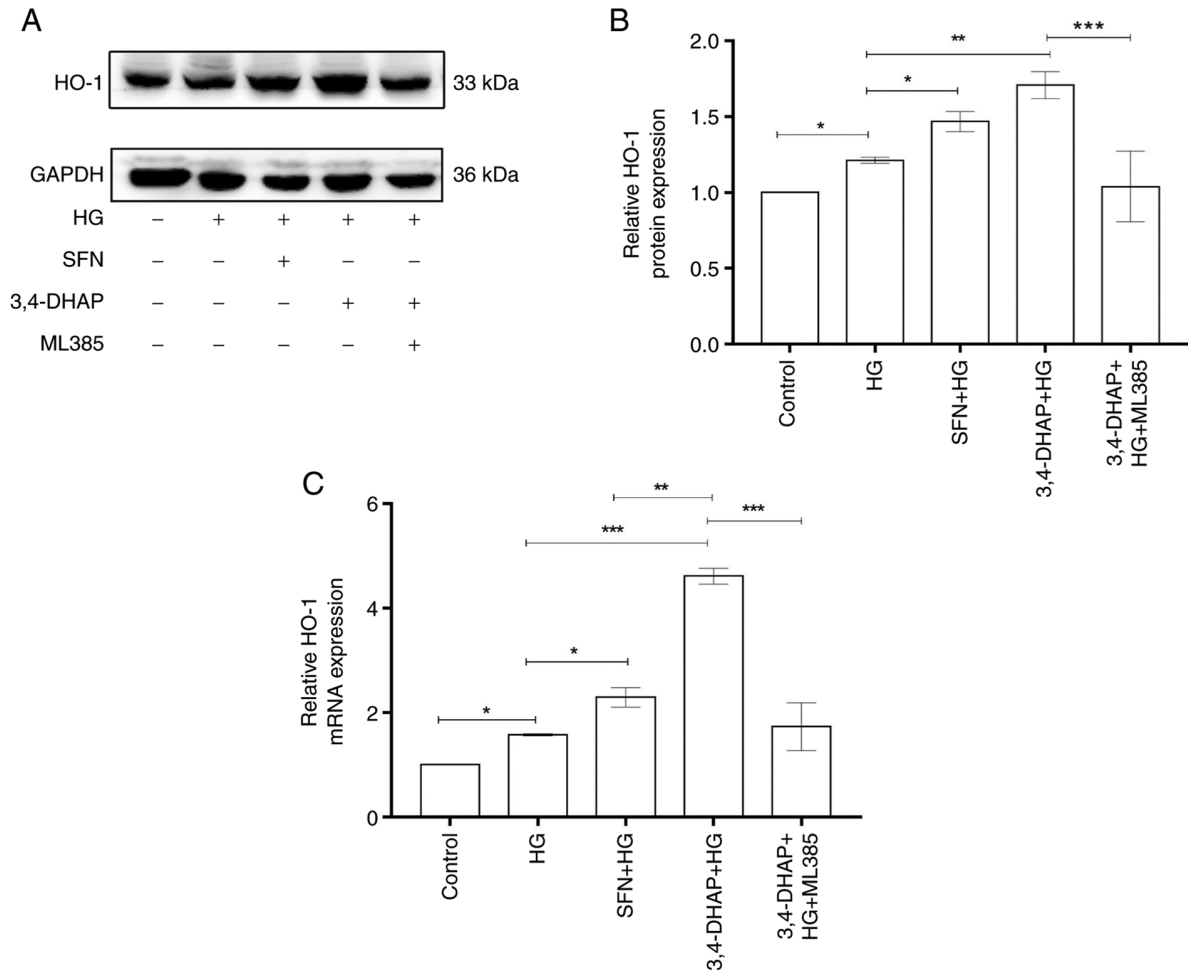


Figure 5. 3,4-DHAP upregulates HO-1 protein and mRNA expression levels. (A) HO-1 protein expression levels were measured using western blotting and (B) quantified using ImageJ software. (C) HO-1 mRNA expression levels. Data are presented as the mean \pm SD of three repeats. * P <0.05, ** P <0.01 and *** P <0.001. 3,4-DHAP, 3,4-dihydroxyacetophenone; HO-1, heme-oxygenase-1; HG, high glucose; SFN, sulforaphane.

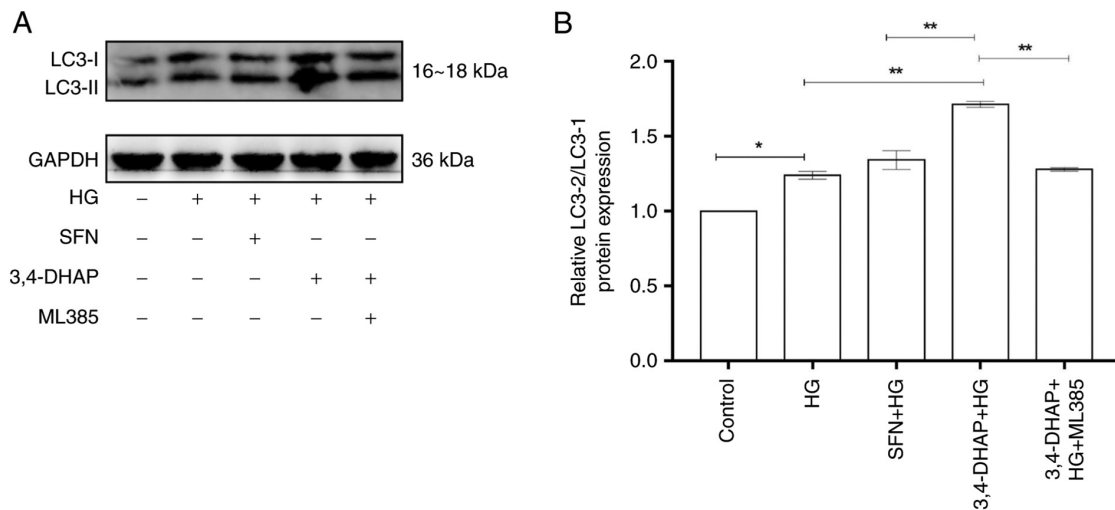


Figure 6. 3,4-DHAP upregulates LC3 protein expression. (A) LC3 protein expression levels were measured by western blotting and (B) the LC3II/LC3I ratio was quantified using ImageJ software. Data are presented as the mean \pm SD of three repeats. * P <0.05 and ** P <0.01. 3,4-DHAP, 3,4-dihydroxyacetophenone; LC3, microtubule-associated protein 1A/1B-light chain 3; HG, high glucose; SFN, sulforaphane.

and hypertension (45). Oxidative stress is a state that arises following an imbalance between oxidation and antioxidation. Vascular oxidative stress promotes endothelial dysfunction

and atherosclerotic progression (46). Oxidative stress induced by high glucose levels is a major factor in diabetic macroangiopathy (47). Therefore, a model of diabetes was established

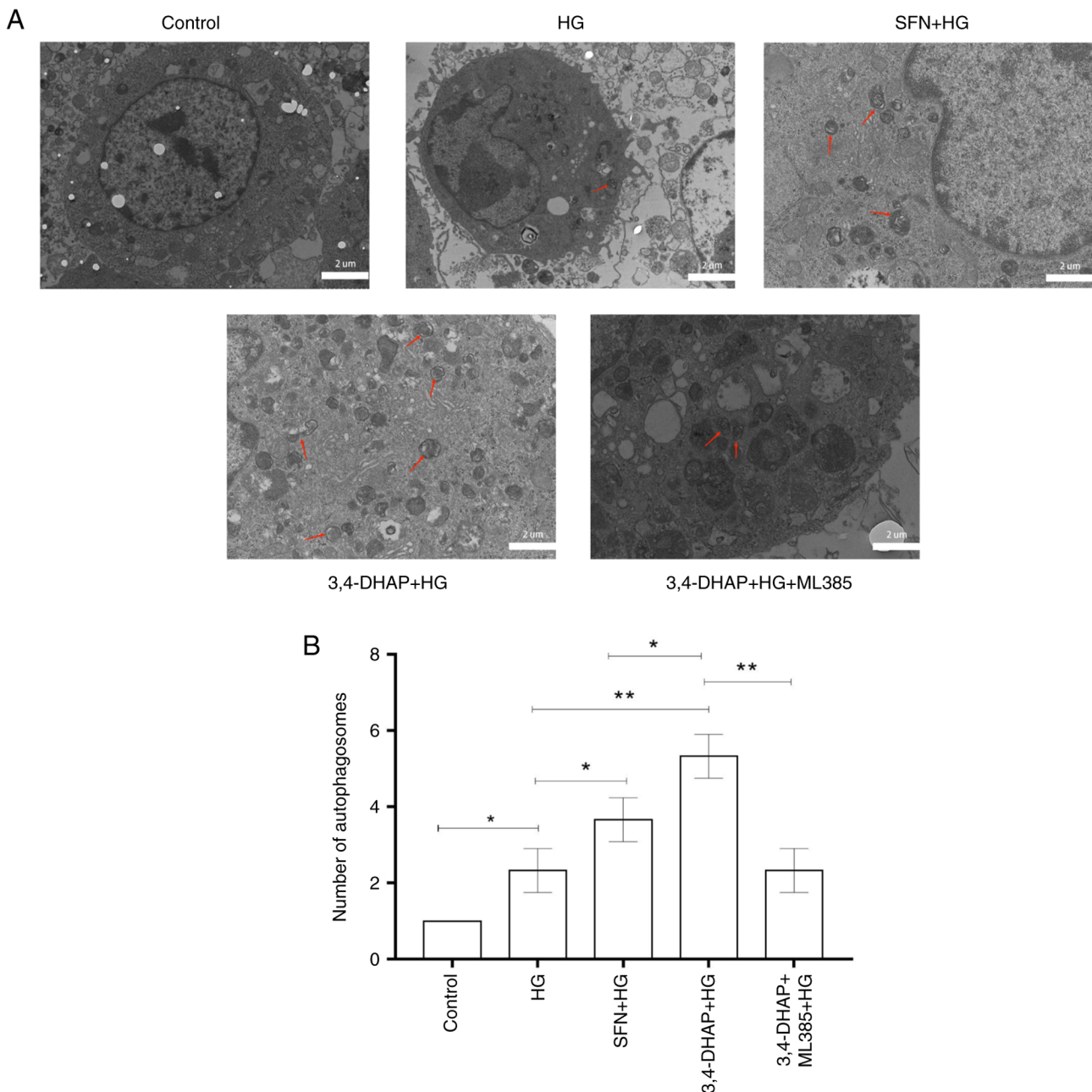


Figure 7. 3,4-DHAP promotes the formation of autophagosomes. (A) Autophagosomes are captured by TEM and shown using a red arrow. (B) The number of autophagosomes was quantified using ImageJ software. Data are presented as the mean \pm SD of three repeats. * $P<0.05$ and ** $P<0.01$. 3,4-DHAP, 3,4-dihydroxyacetophenone; TEM, transmission electron microscope; HG, high glucose; SFN, sulforaphane.

using high glucose medium. The results also showed that there was a significant reduction in cell viability in cells cultured under high glucose conditions.

ROS homeostasis in the majority of organisms is maintained through the balance between ROS production and ROS scavenging (48). When there is an imbalance between generation and reduction of ROS, ROS levels are increased. Increased ROS levels leads to a disorder of the antioxidant system and accumulation of ROS, resulting in an oxidative stress (49). Excessive ROS levels notably alter the function of endothelial cells, such as causing metabolic imbalances and oxidative stress (50), affecting mitochondrial morphology and function (51) and inducing autophagy and cell death (52). There are numerous studies that have suggested that the levels

of ROS exert a potent effect in the occurrence of oxidative stress (53-55). Similarly, in the present study, ROS production was markedly increased in the high glucose group compared with the control group.

ROS can be eliminated through antioxidant effects. Zhong *et al* (56) showed that the defense function of the cell was activated by the increase in ROS levels when cells were damaged, thus cellular antioxidant mechanisms are activated and upregulated to scavenge the ROS. Das *et al* (57) reported that persistent hyperglycemia impaired the pro-oxidant and antioxidant balance, which in-turn reduced antioxidant levels and increased ROS production under diabetic conditions. Wang *et al* (58) indicated that baicalein (BL) increased production of ROS or decreased the expression of antioxidant

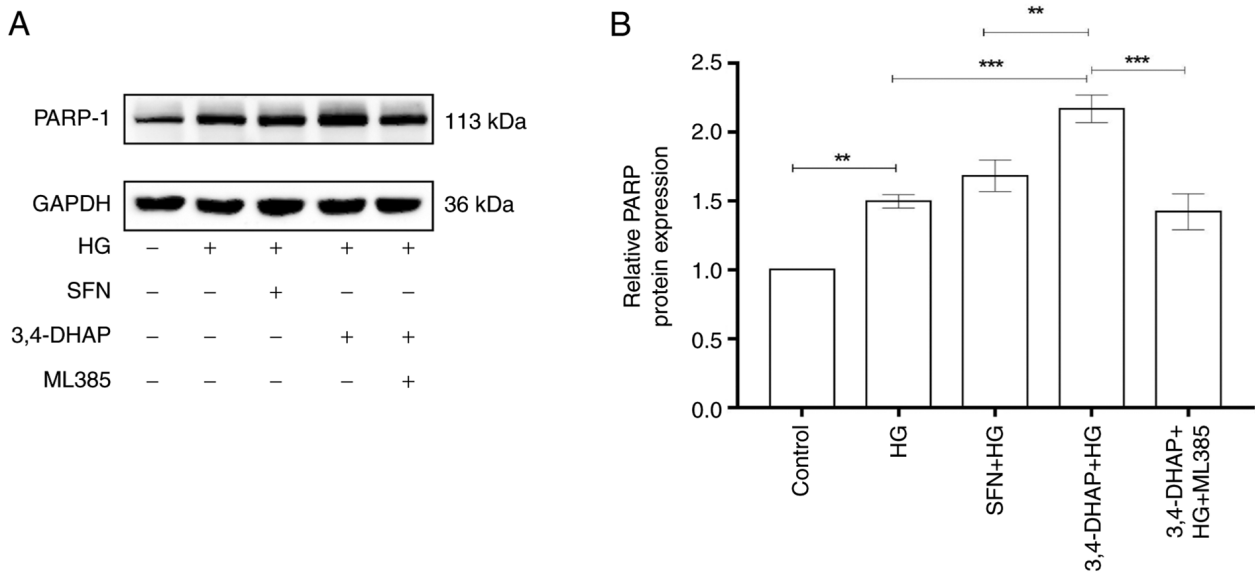


Figure 8. 3,4-DHAP upregulates PARP protein expression levels. (A) PARP protein expression levels were measured using western blotting and (B) quantified using ImageJ software. Data are presented as the mean \pm SD of three repeats. ** $P < 0.01$ and *** $P < 0.001$. 3,4-DHAP, 3,4-dihydroxyacetophenone; PARP, poly-ADP ribose polymerase; HG, high glucose; SFN, sulforaphane.

proteins mediated by ROS, to promote cancer cell death. 3,4-DHAP, a compound extracted from *Ilex glauca* leaves, has physiological activities and beneficial effects for cardiovascular diseases with relatively little toxicity and few side effects (38). It also has a therapeutic effect on coronary heart diseases, angina pectoris and pregnancy hypertension (59), and has been clinically adopted as a novel treatment for coronary heart diseases and angina pectoris. Wu *et al* (60) suggested that 3,4-DHAP exerted anti-inflammatory function on LPS-activated macrophages. Lu and Chen (37) showed that 3,4-DHAP could eliminate free radicals and increase resistance to lipid peroxidation to protect the function of the brain. The present study showed that 3,4-DHAP increased cell viability and markedly reduced ROS levels compared with the high glucose group. Thus, 3,4-DHAP was hypothesized to exhibit a potent antioxidant effect and to attenuate oxidative stress induced by high glucose in HUVECs.

It is well established that Nrf2 is the primary defense mechanism against cellular oxidative stress (61). When an antioxidant stimulates a cell, Nrf2 becomes decoupled from the cytoplasmic protein chaperone molecule Keap1 and enters the nucleus, where it binds to the antioxidant reaction element (ARE) to eliminate ROS (62). HO-1, an important antioxidant enzyme, primarily catalyzes hemoglobin into ferrous iron, carbon monoxide and biliverdin. The degradation of the heme group is conducive in preventing its oxidative promotion. When Nrf2 is present in the nucleus, HO-1 promoter activity is regulated by Nrf2. Furthermore, the activation of the Nrf2/HO-1 pathway exerts a potent effect on cells, especially when under conditions of oxidative stress (63). Martinez *et al* (64) demonstrated that BML-111 could increase Nrf2, HO-1 and NQO1 expression levels to lower oxidative stress induced by ultraviolet radiation B (UVB). Piao *et al* (65) also showed that the Nrf2 and HO-1 levels were upregulated after treatment with mangiferin (MF), suggesting that the antioxidant effects of MF were regulated

by Nrf2/HO-1. A previous study has shown that Nrf2 expression is increased as well as its translocation to the nucleus, and this plays a pivotal role in its antioxidant effects (66). In the present study, Nrf2 and HO-1 protein and mRNA expression levels in the 3,4-DHAP group were higher than that in the high glucose group. The Nrf2 nuclear levels were enhanced in cells pretreated with 3,4-DHAP when compared with the high glucose group. Thus, it was considered that 3,4-DHAP may exert an antioxidant role by regulating the Nrf2/HO-1 pathway to eliminate excessive ROS.

In addition, ML385, the Nrf2 activity inhibitor, could directly interact with the Nrf2 protein, binding to the Neh1 binding region of Nrf2, thus preventing the establishment of the Nrf2-mafg complex at ARE promoter sequences and in-turn reducing transcriptional activity. In lung cancer cells, ML385 targeted Nrf2 signaling, affected colony formation ability and the growth of cells, as well as Nrf2-mediated functions (67). Liu *et al* (68) confirmed that the protective effects of isoliquiritigenin on acute pancreatitis in mice were mediated through inhibition of oxidative stress and modulation of the Nrf2/HO-1 pathway. Thus, in order to determine whether 3,4-DHAP exerted its antioxidant effects through the Nrf2/HO-1 pathway, ML385 was used to inhibit Nrf2. The results showed that compared with the 3,4-DHAP group, the Nrf2 total and nuclear protein levels in the 3,4-DHAP + ML385 group were decreased, the mRNA expression levels of Nrf2 in the 3,4-DHAP + ML385 group were reduced, and the HO-1 protein and mRNA expression levels in the 3,4-DHAP + ML385 group were also reduced. These findings further suggested that 3,4-DHAP protected HUVECs from oxidative stress induced by high glucose through the Nrf2/HO-1 pathway. However, HO-1 is one of numerous downstream genes regulated by Nrf2; other downstream genes such as NQO1, GCLC, GCLM may have also participated in the oxidative protective mechanisms in the HUVECs treated with high glucose (69). The involvement of other genes will be assessed in future studies.

Autophagy is a biological process in which damaged organelles, misfolded proteins and invading pathogens are enveloped in an intracellular double-membraned structure and degraded. When stimulated by stressors such as starvation, hypoxia, infection and DNA damage (70), autophagy is further activated and plays a protective role by removing abnormal organelles (71). Growing evidence supports the notion that a series of biological factors and compounds can induce vascular endothelial cells to undergo autophagy to resist stress responses and protect the cell. Xu *et al* (72) found that rapamycin activated autophagy and reduced DNA radiation damage of bone marrow blood cells through the STAT3 signaling pathway. However, when autophagy was over-activated, it resulted in autophagic death (73). Studies have shown that treatment of endothelial cells with endostatin, an endogenous angiogenic inhibitor, induced autophagy and cell death (74,75). LC3 is a specific marker for autophagosome formation (76). LC3 was previously considered to be involved in the regulation of microtubule assembly and disassembly. Subsequently, LC3 was found to exert specific autophagic effects. During the formation of autophagosomes, LC3-I is transformed into LC3-II by binding to phosphatidylethanolamine. When the LC3-II/LC3-I ratio increases, this is indicative that autophagy has occurred. Qiao *et al* (77) found that the anticancer effects of TRAIL were increased following azithromycin treatment, which may be related to LC3-mediated autophagy. A previous study has shown that aminoguanidine (AG) reduces the LC3-II/LC3-I ratio and ROS production to inhibit autophagy (78). The autophagosome, a key structure in the process of autophagy, envelops damaged organelles or proteins and combines with lysosomes to generate an autophagolysosome. Liang *et al* (79) observed that autophagosomes were formed in the early stages of autophagy and matured in the later stages of autophagy. In the present study, the protein expression levels of LC3-II/LC3-I and the formation of autophagosomes in the high glucose group was slightly increased compared with the control group. This demonstrated that autophagy was activated when stimulated by oxidation. Furthermore, 3,4-DHAP markedly enhanced LC3-II/LC3-I protein levels and the formation of autophagosomes compared with the high glucose group. Therefore, it was suggested that 3,4-DHAP could protect HUVECs from oxidative stress by enhancing autophagy levels.

The stability of genomic DNA is vital for the survival of individuals and the long-term reproduction of species. When DNA damage occurs, cells need to activate the DNA damage repair mechanisms, and the cell cycle is arrested, preventing the cell in question from continuing mitosis. After the DNA damage is repaired, the cell cycle is resumed and the cell begins to undergo mitosis again (80). The working system of DNA damage repair includes sensors, mediators, signal transmitters and effectors (81). The receptors primarily involved in this process are PARP1/2, the 9-1-1 complex and the RAD17-RFC complex (82,83). PARP-1 is a multifunctional protein that post-translationally modifies enzymes already present in the majority eukaryotic cells. PARP-1 can sense DNA damage and is activated by identifying DNA fragments with structural damage. Studies have shown that PARP inhibitors cause an increase in DNA damage and prevent cells from repairing single-stranded DNA breaks (84). Therefore, PARP-1 plays a significant role in DNA damage repair and transcriptional

regulation (85). Isakoff *et al* (86) discovered that DNA damage repair was blocked by PARP inhibitors, and the clinical activity of DNA-damaging chemotherapy was enhanced when combined with these inhibitors. The results of the present study showed that 3,4-DHAP markedly enhanced PARP-1 protein expression levels compared with the high glucose group. In short, these findings demonstrated that 3,4-DHAP could promote DNA repair in HUVECs by regulating the expression of PARP-1.

An increasing number of studies have found that the mutual regulation between autophagy and Nrf2 is involved in modulation of ROS and other factors. ROS plays a critical role in autophagy. Pajares *et al* (87) found that Nrf2 regulated autophagy gene transcription in a mouse model of Alzheimer's disease. Feng *et al* (88) showed that activating the Nrf2 pathway could upregulate autophagy to protect LPS-induced HK-2 cell injury. In the present study, a possible association between Nrf2 and autophagy was identified. Compared with the 3,4-DHAP group, the protein expression levels of LC3-II/LC3-I were reduced in the 3,4-DHAP + ML385 group. Therefore, it was hypothesized that Nrf2 may induce autophagy to repair damaged endothelial cells. Furthermore, autophagy was involved in the repair of damaged DNA in cells (89). Studies have suggested that PARP-1 has a profound effect on autophagy and is an important indicator in the formation and maturation of autophagosomes (90). Rodríguez-Vargas *et al* (91) showed that the production of ROS led to DNA damage and excessive activation of PARP-1 when autophagy was induced by starvation. Thus, in the present study, it was hypothesized that there was a link between autophagy and DNA damage. The protein expression levels of PARP were reduced in the 3,4-DHAP + ML385 group compared with the 3,4-DHAP group. However, the mechanisms linking autophagy and Nrf2, and linking autophagy and DNA damage repair require further study to elucidate.

In the present study it was determined that 3,4-DHAP treatment reduced ROS production, upregulated Nrf2 protein and mRNA expression, increased HO-1 protein and mRNA expression, promoted Nrf2 nuclear translocation, increased LC3-II/LC3-I and PARP-1 protein expression and promoted the formation of autophagosomes. At present, the prevention and treatment of T2DM and its complications are still a major problem to be solved in China. Clinically, drugs for the comprehensive treatment of diabetes and AS are still in short supply. The present study found that 3,4-DHAP has an inhibitory effect on inflammatory response and oxidative stress. Therefore, 3,4-DHAP may be the drug of choice for treatment. However, the current experimental study has limitations. We are currently investigating the protective effect of 3,4-DHAP on HUVECs and its molecular mechanism, which needs to be verified *in vivo*. Regarding autophagy and DNA damage repair, only 3,4-DHAP has been studied to regulate autophagy and DNA damage repair, and its mechanism needs to be further studied. In addition, the manner in which 3,4-DHAP regulates Nrf2, autophagy and DNA repair is also a problem to be solved in the next experimental stage. In conclusion, the results suggest that 3,4-DHAP possesses antioxidative properties and was thus able to protect HUVECs from oxidative stress via regulation of the Nrf2/HO-1 pathway, enhancing autophagy and promoting DNA damage repair.

Acknowledgements

Not applicable.

Funding

This work was supported by the Shandong Natural Science Foundation (grant nos. ZR2020MH415 and ZR2021LZY033).

Availability of data and materials

The datasets used and/or analyzed during the current study are available from the corresponding author on reasonable request.

Authors' contributions

DZ, JL and DC conceived and designed the study. DC and YW performed the experiments. DC drafted the manuscript. WL, YW, JJ, and JG performed data analysis. DZ and JL were responsible for data interpretation. WL, JJ and JG revised the manuscript critically for important intellectual content. DZ, JL and DC confirm the authenticity of all the raw data. All authors have read and approved the final manuscript.

Ethics approval and consent to participate

Not applicable.

Patient consent for publication

Not applicable.

Competing interests

The authors declare that they have no competing interests.

References

1. Cho NH, Shaw JE, Karuranga S, Huang Y, da Rocha Fernandes JD, Ohlrogge AW and Malanda B: IDF diabetes atlas: Global estimates of diabetes prevalence for 2017 and projections for 2045. *Diabetes Res Clin Pract* 138: 271-281, 2018.
2. Newman JD, Schwartzbard AZ, Weintraub HS, Goldberg JJ and Berger JS: Primary prevention of cardiovascular disease in diabetes mellitus. *J Am Coll Cardiol* 70: 883-893, 2017.
3. Sheng B, Truong K, Spitler H, Zhang L, Tong X and Chen L: The long-term effects of bariatric surgery on type 2 diabetes remission, microvascular and macrovascular complications, and mortality: A systematic review and meta-analysis. *Obes Surg* 27: 2724-2732, 2017.
4. GBD 2016 Causes of Death Collaborators: Global, regional, and national age-sex specific mortality for 264 causes of death, 1980-2016: A systematic analysis for the Global Burden of Disease Study 2016. *Lancet* 390: 1151-1210, 2017.
5. Luo JF, Shen XY, Lio CK, Dai Y, Cheng CS, Liu JX, Yao YD, Yu Y, Xie Y, Luo P, *et al.*: Activation of Nrf2/HO-1 pathway by nardochinoid C inhibits inflammation and oxidative stress in lipopolysaccharide-stimulated macrophages. *Front Pharmacol* 9: 911, 2018.
6. Zuo L, Prather ER, Stetskiy M, Garrison DE, Meade JR, Peace TI and Zhou T: Inflammaging and oxidative stress in human diseases: From molecular mechanisms to novel treatments. *Int J Mol Sci* 20: 4472, 2019.
7. Förstermann U, Xia N and Li H: Roles of vascular oxidative stress and nitric oxide in the pathogenesis of atherosclerosis. *Circ Res* 120: 713-735, 2017.
8. Costa JG, Saraiva N, Batinic-Haberle I, Castro M, Oliveira NG and Fernandes AS: The SOD Mimic MnTnHex-2-PyP³⁺ reduces the viability and migration of 786-O human renal cancer cells. *Antioxidants (Basel)* 8: 490, 2019.
9. Ge C, Tan J, Zhong S, Lai L, Chen G, Zhao J, Yi C, Wang L, Zhou L, Tang T, *et al.*: Nrf2 mitigates prolonged PM2.5 exposure-triggered liver inflammation by positively regulating SIKE activity: Protection by Juglanin. *Redox Biol* 36: 101645, 2020.
10. Rojo de la Vega M, Chapman E and Zhang DD: NRF2 and the hallmarks of cancer. *Cancer Cell* 34: 21-43, 2018.
11. Suzuki T, Motohashi H and Yamamoto M: Toward clinical application of the Keap1-Nrf2 pathway. *Trends Pharmacol Sci* 34: 340-346, 2013.
12. Leinonen HM, Kansanen E, Pölonen P, Heinäniemi M and Levenon AL: Role of the Keap1-Nrf2 pathway in cancer. *Adv Cancer Res* 122: 281-320, 2014.
13. Cuadrado A, Rojo AI, Wells G, Hayes JD, Cousin SP, Rumsey WL, Attucks OC, Franklin S, Levenon AL, Kensler TW and Dinkova-Kostova AT: Therapeutic targeting of the NRF2 and KEAP1 partnership in chronic diseases. *Nat Rev Drug Discov* 18: 295-317, 2019.
14. Kobayashi A, Kang MI, Okawa H, Ohtsuji M, Zenke Y, Chiba T, Igarashi K and Yamamoto M: Oxidative stress sensor Keap1 functions as an adaptor for Cul3-based E3 ligase to regulate proteasomal degradation of Nrf2. *Mol Cell Biol* 24: 7130-7139, 2004.
15. Warabi E, Takabe W, Minami T, Inoue K, Itoh K, Yamamoto M, Ishii T, Kodama T and Noguchi N: Shear stress stabilizes NF-E2-related factor 2 and induces antioxidant genes in endothelial cells: Role of reactive oxygen/nitrogen species. *Free Radic Biol Med* 42: 260-269, 2007.
16. Farkhondeh T, Pourbagher-Shahri AM, Azimi-Nezhad M, Forouzanfar F, Brockmueller A, Ashrafizadeh M, Talebi M, Shakibaei M and Samarghandian S: Roles of Nrf2 in gastric cancer: Targeting for therapeutic strategies. *Molecules* 26: 3157, 2021.
17. Su L, Cao P and Wang H: Tetrandrine mediates renal function and redox homeostasis in a streptozotocin-induced diabetic nephropathy rat model through Nrf2/HO-1 reactivation. *Ann Transl Med* 8: 990, 2020.
18. Zhang S, Li T, Zhang L, Wang X, Dong H, Li L, Fu D, Li Y, Zi X, Liu HM, *et al.*: A novel chalcone derivative S17 induces apoptosis through ROS dependent DR5 up-regulation in gastric cancer cells. *Sci Rep* 7: 9873, 2017.
19. Ci X, Lv H, Wang L, Wang X, Peng L, Qin FX and Cheng G: The antioxidative potential of farrerol occurs via the activation of Nrf2 mediated HO-1 signaling in RAW 264.7 cells. *Chem Biol Interact* 239: 192-199, 2015.
20. Mohammad J, Singh RR, Riggall C, Haugrud B, Abdalla MY and Reindl KM: JNK inhibition blocks piperlongumine-induced cell death and transcriptional activation of heme oxygenase-1 in pancreatic cancer cells. *Apoptosis* 24: 730-744, 2019.
21. Levine B and Kroemer G: Autophagy in the pathogenesis of disease. *Cell* 132: 27-42, 2008.
22. Hu B, Zhang Y, Jia L, Wu H, Fan C, Sun Y, Ye C, Liao M and Zhou J: Binding of the pathogen receptor HSP90AA1 to avibirnavirus VP2 induces autophagy by inactivating the AKT-MTOR pathway. *Autophagy* 11: 503-515, 2015.
23. Zhao YG, Codogno P and Zhang H: Machinery, regulation and pathophysiological implications of autophagosome maturation. *Nat Rev Mol Cell Biol* 22: 733-750, 2021.
24. Laverdure S, Wang Z, Yang J, Yamamoto T, Thomas T, Sato T, Nagashima K and Imamichi T: Interleukin-27 promotes autophagy in human serum-induced primary macrophages via an mTOR- and LC3-independent pathway. *Sci Rep* 11: 14898, 2021.
25. Rakovic A, Shurkewitsch K, Seibler P, Grünwald A, Zanon A, Hagenah J, Krainc D and Klein C: Phosphatase and tensin homolog (PTEN)-induced putative kinase 1 (PINK1)-dependent ubiquitination of endogenous Parkin attenuates mitophagy: Study in human primary fibroblasts and induced pluripotent stem cell-derived neurons. *J Biol Chem* 288: 2223-2237, 2013.
26. Yang A, Pantoom S and Wu YW: Elucidation of the anti-autophagy mechanism of the Legionella effector RavZ using semisynthetic LC3 proteins. *Elife* 6: e23905, 2017.
27. Han X, Liu JX and Li XZ: Salvianolic acid B inhibits autophagy and protects starving cardiac myocytes. *Acta Pharmacol Sin* 32: 38-44, 2011.
28. Mikolaskova B, Jurcik M, Cipakova I, Kretova M, Chovanec M and Cipak L: Maintenance of genome stability: The unifying role of interconnections between the DNA damage response and RNA-processing pathways. *Curr Genet* 64: 971-983, 2018.

29. Wang Y, Luo W and Wang Y: PARP-1 and its associated nucleases in DNA damage response. *DNA Repair (Amst)* 81: 102651, 2019.
30. Zhou Y, Tang S, Chen T and Niu MM: Structure-based pharmacophore modeling, virtual screening, molecular docking and biological evaluation for identification of potential poly (ADP-Ribose) Polymerase-1 (PARP-1) Inhibitors. *Molecules* 24: 4258, 2019.
31. Schiewer MJ, Mandigo AC, Gordon N, Huang F, Gaur S, de Leeuw R, Zhao SG, Evans J, Han S, Parsons T, *et al*: PARP-1 regulates DNA repair factor availability. *EMBO Mol Med* 10: e8816, 2018.
32. Pazzaglia S and Pioli C: Multifaceted Role of PARP-1 in DNA repair and inflammation: Pathological and therapeutic implications in cancer and non-cancer diseases. *Cells* 9: 41, 2019.
33. Liu Y, Song H, Song H, Feng X, Zhou C and Huo Z: Targeting autophagy potentiates the anti-tumor effect of PARP inhibitor in pediatric chronic myeloid leukemia. *AMB Express* 9: 108, 2019.
34. Wang L, Wei W, Xiao Q, Yang H and Ci X: Farrerol Ameliorates APAP-induced hepatotoxicity via activation of Nrf2 and autophagy. *Int J Biol Sci* 15: 788-799, 2019.
35. Fan SF, Zhou NH, Hu SL and Xu SG: Effects of 3,4-dihydroxyacetophenone in shortening of action potential duration of cardiac cells (author's transl). *Zhongguo Yao Li Xue Bao* 2: 107-110, 1981 (In Chinese).
36. Kim YJ, No JK, Lee JS, Kim MS and Chung HY: Antimelanogenic activity of 3,4-dihydroxyacetophenone: Inhibition of tyrosinase and MITF. *Biosci Biotechnol Biochem* 70: 532-534, 2006.
37. Lu XY and Chen WC: Effect of 3, 4-dihydroxyacetophenone on Na⁺, K⁺-ATPase activity of injured mitochondria and the oxygen consumption of brain cells of rat. *Yao Xue Xue Bao* 40: 13-16, 2005.
38. Zhang D, Liu J, Wang L, Wang J, Li W, Zhuang B, Hou J and Liu T: Effects of 3,4-dihydroxyacetophenone on the hypercholesterolemia-induced atherosclerotic rabbits. *Biol Pharm Bull* 36: 733-740, 2013.
39. Livak KJ and Schmittgen TD: Analysis of relative gene expression data using real-time quantitative PCR and the 2(-Delta Delta C(T)) method. *Methods* 25: 402-408, 2001.
40. Aranda A, Sequedo L, Tolosa L, Quintas G, Burello E, Castell JV and Gombau L: Dichloro-dihydro-fluorescein diacetate (DCFH-DA) assay: A quantitative method for oxidative stress assessment of nanoparticle-treated cells. *Toxicol In Vitro* 27: 954-963, 2013.
41. Arakawa S, Honda S, Yamaguchi H and Shimizu S: Molecular mechanisms and physiological roles of Atg5/Atg7-independent alternative autophagy. *Proc Jpn Acad Ser B Phys Biol Sci* 93: 378-385, 2017.
42. Dunphy G, Flannery SM, Almine JF, Connolly DJ, Paulus C, Jönsson KL, Jakobsen MR, Nevels MM, Bowie AG and Unterholzner L: Non-canonical activation of the DNA sensing adaptor STING by ATM and IFI16 mediates NF-κB signaling after nuclear DNA damage. *Mol Cell* 71: 745-760.e5, 2018.
43. Hemmingsen B, Gimenez-Perez G, Mauricio D, Roqué IFM, Metzendorf MI and Richter B: Diet, physical activity or both for prevention or delay of type 2 diabetes mellitus and its associated complications in people at increased risk of developing type 2 diabetes mellitus. *Cochrane Database Syst Rev*: Dec 4, 2017 (Epub ahead of print).
44. Wu Y, Song F, Li Y, Li J, Cui Y, Hong Y, Han W, Wu W, Lakhani I, Li G and Wang Y: Acacetin exerts antioxidant potential against atherosclerosis through Nrf2 pathway in apoE(-/-) Mice. *J Cell Mol Med* 25: 521-534, 2021.
45. Kaur R, Kaur M and Singh J: Endothelial dysfunction and platelet hyperactivity in type 2 diabetes mellitus: Molecular insights and therapeutic strategies. *Cardiovasc Diabetol* 17: 121, 2018.
46. Sena CM, Leandro A, Azul L, Seica R and Perry G: Vascular oxidative stress: Impact and therapeutic approaches. *Front Physiol* 9: 1668, 2018.
47. Jiao B, Wang YS, Cheng YN, Gao JJ and Zhang QZ: Valsartan attenuated oxidative stress, decreased MCP-1 and TGF-β1 expression in glomerular mesangial and epithelial cells induced by high-glucose levels. *Biosci Trends* 5: 173-181, 2011.
48. Wang M, Sun X, Yu D, Xu J, Chung K and Li H: Genomic and transcriptomic analyses of the tangerine pathotype of *Alternaria alternata* in response to oxidative stress. *Sci Rep* 6: 32437, 2016.
49. Guo J, Zhao MH, Shin KT, Niu YJ, Ahn YD, Kim NH and Cui XS: The possible molecular mechanisms of bisphenol A action on porcine early embryonic development. *Sci Rep* 7: 8632, 2017.
50. An J, Li Q, Yang J, Zhao Z, Wu Y, Wang Y and Wang W: Wheat F-box protein TaFBA1 positively regulates plant drought tolerance but negatively regulates stomatal closure. *Front Plant Sci* 10: 1242, 2019.
51. Zhang R, Liu B, Fan X, Wang W, Xu T, Wei S, Zheng W, Yuan Q, Gao L, Yin X, *et al*: Aldehyde dehydrogenase 2 protects against post-cardiac arrest myocardial dysfunction through a novel mechanism of suppressing mitochondrial reactive oxygen species production. *Front Pharmacol* 11: 373, 2020.
52. Bazhin AV, Philippov PP and Karakhanova S: Reactive oxygen species in cancer biology and anticancer therapy. *Oxid Med Cell Longev* 2016: 4197815, 2016.
53. Senoner T and Dichtl W: Oxidative stress in cardiovascular diseases: Still a therapeutic target? *Nutrients* 11: 2090, 2019.
54. Kang Q and Yang C: Oxidative stress and diabetic retinopathy: Molecular mechanisms, pathogenetic role and therapeutic implications. *Redox Biol* 37: 101799, 2020.
55. Shah MS and Brownlee M: Molecular and cellular mechanisms of cardiovascular disorders in diabetes. *Circ Res* 118: 1808-1829, 2016.
56. Zhong Z, Fu X, Li H, Chen J, Wang M, Gao S, Zhang L, Cheng C, Zhang Y, Li P, *et al*: Citicoline protects auditory hair cells against neomycin-induced damage. *Front Cell Dev Biol* 8: 712, 2020.
57. Das SK, Prusty A, Samantaray D, Hasan M, Jena S, Patra JK, Samanta L and Thatoi H: Effect of *Xylocarpus granatum* bark extract on amelioration of hyperglycaemia and oxidative stress associated complications in STZ-induced diabetic mice. *Evid Based Complement Alternat Med* 2019: 8493190, 2019.
58. Wang SX, Wen X, Bell C and Appiah S: Liposome-delivered baicalein induction of myeloid leukemia K562 cell death via reactive oxygen species generation. *Mol Med Rep* 17: 4524-4530, 2018.
59. Yang DS, Xi-Rui W and Ting-Yuan M: Effects of 3,4-dihydroxyacetophenone on the biosynthesis of TXA2 and PGI2 in human placental villus and umbilical artery segments in vitro. *Prostaglandins* 38: 497-504, 1989.
60. Wu P, Ye D, Zhang D, Zhang L, Wan J and Pan Q: Dual effect of 3,4-dihydroxyacetophenone on LPS-induced apoptosis in RAW264.7 cells by modulating the production of TNF-α. *J Huazhong Univ Sci Technolog Med Sci* 25: 131-134, 2005.
61. Fan X, Wei W, Huang J, Liu X and Ci X: Isoorientin attenuates cisplatin-induced nephrotoxicity through the inhibition of oxidative stress and apoptosis via activating the SIRT1/SIRT6/Nrf-2 pathway. *Front Pharmacol* 11: 264, 2020.
62. Qin JJ, Cheng XD, Zhang J and Zhang WD: Dual roles and therapeutic potential of Keap1-Nrf2 pathway in pancreatic cancer: A systematic review. *Cell Commun Signal* 17: 121, 2019.
63. Li T, Chen B, Du M, Song J, Cheng X, Wang X and Mao X: Casein glycomacropeptide hydrolysates exert cytoprotective effect against cellular oxidative stress by Up-Regulating HO-1 expression in HepG2 cells. *Nutrients* 9: 31, 2017.
64. Martinez RM, Fattori V, Saito P, Pinto IC, Rodrigues CCA, Melo CPB, Bussmann AJC, Staurengo-Ferrari L, Bezerra JR, Vignoli JA, *et al*: The lipoxin Receptor/FPR2 agonist BML-111 protects mouse skin against ultraviolet B radiation. *Molecules* 25: 2953, 2020.
65. Piao CH, Fan YJ, Nguyen TV, Song CH and Chai OH: Mangiferin alleviates ovalbumin-induced allergic rhinitis via Nrf2/HO-1/NF-κB signaling pathways. *Int J Mol Sci* 21: 3415, 2020.
66. Probst BL, McCauley L, Trevino I, Wigley WC and Ferguson DA: Cancer cell growth is differentially affected by constitutive activation of NRF2 by KEAP1 deletion and pharmacological activation of NRF2 by the synthetic triterpenoid, RTA 405. *PLoS One* 10: e0135257, 2015.
67. Singh A, Venkannagari S, Oh KH, Zhang YQ, Rohde JM, Liu L, Nimmagadda S, Sudini K, Brimacombe KR, Gajghate S, *et al*: Small molecule inhibitor of NRF2 selectively intervenes therapeutic resistance in KEAP1-deficient NSCLC tumors. *ACS Chem Biol* 11: 3214-3225, 2016.
68. Liu X, Zhu Q, Zhang M, Yin T, Xu R, Xiao W, Wu J, Deng B, Gao X, Gong W, *et al*: Isoliquiritigenin ameliorates acute pancreatitis in mice via inhibition of oxidative stress and modulation of the Nrf2/HO-1 pathway. *Oxid Med Cell Longev* 2018: 7161592, 2018.
69. Zhao Y, Sun Y, Wang G, Ge S and Liu H: Dendrobium officinale polysaccharides protect against MNNG-Induced PLGC in rats via activating the NRF2 and antioxidant enzymes HO-1 and NQO-1. *Oxid Med Cell Longev* 2019: 9310245, 2019.

70. Gomes LR, Menck CFM and Leandro GS: Autophagy roles in the modulation of DNA repair pathways. *Int J Mol Sci* 18: 2351, 2017.
71. Liao SX, Sun PP, Gu YH, Rao XM, Zhang LY and Ou-Yang Y: Autophagy and pulmonary disease. *Ther Adv Respir Dis* 13: 1753466619890538, 2019.
72. Xu F, Li X, Yan L, Yuan N, Fang Y, Cao Y, Xu L, Zhang X, Xu L, Ge C, *et al.*: Autophagy promotes the repair of Radiation-Induced DNA damage in bone marrow hematopoietic cells via enhanced STAT3 signaling. *Radiat Res* 187: 382-396, 2017.
73. Galati S, Boni C, Gerra MC, Lazzaretti M and Buschini A: Autophagy: A player in response to oxidative stress and DNA damage. *Oxid Med Cell Longev* 2019: 5692958, 2019.
74. Poluzzi C, Iozzo RV and Schaefer L: Endostatin and endorepellin: A common route of action for similar angiostatic cancer avengers. *Adv Drug Deliv Rev* 97: 156-173, 2016.
75. Nguyen TM, Subramanian IV, Xiao X, Ghosh G, Nguyen P, Kelekar A and Ramakrishnan S: Endostatin induces autophagy in endothelial cells by modulating Beclin 1 and beta-catenin levels. *J Cell Mol Med* 13: 3687-3698, 2009.
76. Deng W, Long Q, Zeng J, Li P, Yang W, Chen X and Xie J: Mycobacterium tuberculosis PE_PGRS41 enhances the intracellular survival of *M. smegmatis* within macrophages via blocking innate immunity and inhibition of host defense. *Sci Rep* 7: 46716, 2017.
77. Qiao X, Wang X, Shang Y, Li Y and Chen SZ: Azithromycin enhances anticancer activity of TRAIL by inhibiting autophagy and up-regulating the protein levels of DR4/5 in colon cancer cells in vitro and in vivo. *Cancer Commun (Lond)* 38: 43, 2018.
78. Lee JH, Parveen A, Do MH, Kang MC, Yumnam S and Kim SY: Molecular mechanisms of methylglyoxal-induced aortic endothelial dysfunction in human vascular endothelial cells. *Cell Death Dis* 11: 403, 2020.
79. Liang C, Lee JS, Inn KS, Gack MU, Li Q, Roberts EA, Vergne I, Deretic V, Feng P, Akazawa C and Jung JU: Beclin1-binding UVRAG targets the class C Vps complex to coordinate autophagosome maturation and endocytic trafficking. *Nat Cell Biol* 10: 776-787, 2008.
80. Shaltiel IA, Krenning L, Bruinsma W and Medema RH: The same, only different-DNA damage checkpoints and their reversal throughout the cell cycle. *J Cell Sci* 128: 607-620, 2015.
81. Ivy SP, de Bono J and Kohn EC: The 'Pushmi-Pullyu' of DNA REPAIR: Clinical synthetic lethality. *Trends Cancer* 2: 646-656, 2016.
82. He G, Siddik ZH, Huang Z, Koomen J, Kobayashi R, Khokhar AR and Kuang J: Induction of p21 by p53 following DNA damage inhibits both Cdk4 and Cdk2 activities. *Oncogene* 24: 2929-2943, 2005.
83. Bartek J and Lukas J: Mammalian G1- and S-phase checkpoints in response to DNA damage. *Curr Opin Cell Biol* 13: 738-747, 2001.
84. Eckert MA, Orozco C, Xiao J, Javellana M and Lengyel E: The Effects of chemotherapeutics on the ovarian cancer microenvironment. *Cancers (Basel)* 13: 3136, 2021.
85. Min X, Heng H, Yu HL, Dan M, Jie C, Zeng Y, Ning H, Liu ZG, Wang ZY and Lin W: Anticancer effects of 10-hydroxycamptothecin induce apoptosis of human osteosarcoma through activating caspase-3, p53 and cytochrome c pathways. *Oncol Lett* 15: 2459-2464, 2018.
86. Isakoff SJ, Puhalla S, Domchek SM, Friedlander M, Kaufman B, Robson M, Telli ML, Diéras V, Han HS, Garber JE, *et al.*: A randomized Phase II study of veliparib with temozolomide or carboplatin/paclitaxel versus placebo with carboplatin/paclitaxel in BRCA1/2 metastatic breast cancer: Design and rationale. *Future Oncol* 13: 307-320, 2017.
87. Pajares M, Jiménez-Moreno N, García-Yagüe ÁJ, Escoll M, de Ceballos ML, Van Leuven F, Rábano A, Yamamoto M, Rojo AI and Cuadrado A: Transcription factor NFE2L2/NRF2 is a regulator of macroautophagy genes. *Autophagy* 12: 1902-1916, 2016.
88. Feng LX, Zhao F, Liu Q, Peng JC, Duan XJ, Yan P, Wu X, Wang HS, Deng YH and Duan SB: Role of Nrf2 in lipopolysaccharide-induced acute kidney injury: Protection by human umbilical cord blood mononuclear cells. *Oxid Med Cell Longev* 2020: 6123459, 2020.
89. Yang J, Yu J, Li D, Yu S, Ke J, Wang L, Wang Y, Qiu Y, Gao X, Zhang J and Huang L: Store-operated calcium entry-activated autophagy protects EPC proliferation via the CAMKK2-MTOR pathway in ox-LDL exposure. *Autophagy* 13: 82-98, 2017.
90. Lin W, Yin CY, Yu Q, Zhou SH, Chai L, Fan J and Wang WD: Expression of glucose transporter-1, hypoxia inducible factor-1 α and beclin-1 in head and neck cancer and their implication. *Int J Clin Exp Pathol* 11: 3708-3717, 2018.
91. Rodríguez-Vargas JM, Ruiz-Magaña MJ, Ruiz-Ruiz C, Majuelos-Melguizo J, Peralta-Leal A, Rodríguez MI, Muñoz-Gómez JA, de Almodóvar MR, Siles E, Rivas AL, *et al.*: ROS-induced DNA damage and PARP-1 are required for optimal induction of starvation-induced autophagy. *Cell Res* 22: 1181-1198, 2012.



This work is licensed under a Creative Commons Attribution 4.0 International (CC BY-NC 4.0) License